SUPPLEMENTARY INFORMATION

For manuscript

CpG and methylation dependent DNA binding and dynamics of the Methylcytosine Binding Domain 2 protein at the single-molecule level

Hai Pan[1,†], Stephanie M. Bilinovich[2,†], Parminder Kaur[1], Robert Riehn[1], Hong Wang[1,3,*], David C. Williams Jr[2,*]

[1]Department of Physics, North Carolina State University, Raleigh, North Carolina, NC 27695, USA

[2]Department of Pathology and Laboratory Medicine, University of North Carolina at Chapel Hill, Chapel Hill, NC 27599, USA

[3]Center for Human Health and the Environment, North Carolina State University, Raleigh, North Carolina, NC 27695, USA

This Supplementary Information Contains:

Supplementary Figures S1-10

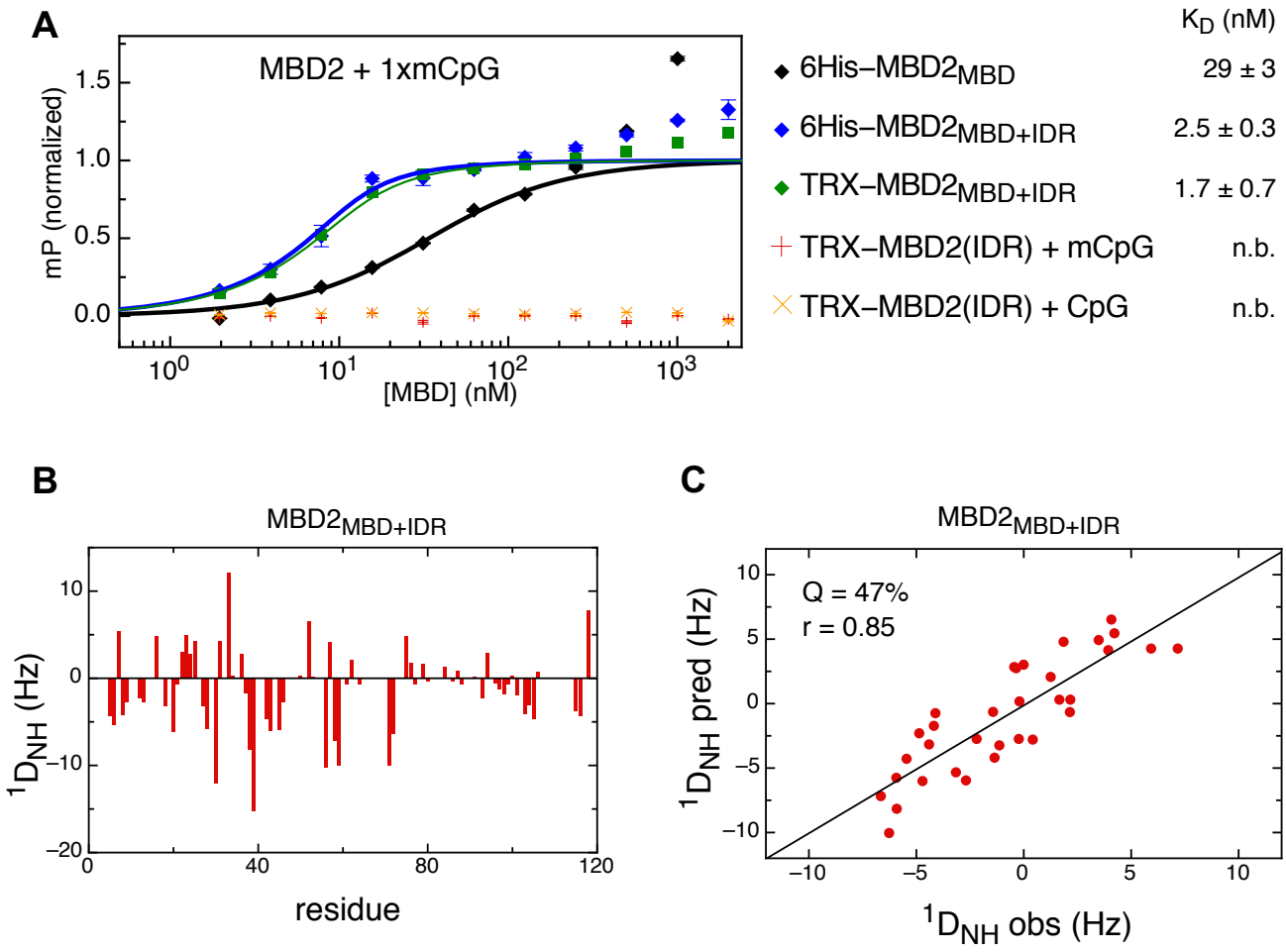

Supplementary Figure S1. Binding affinity and NMR analyses of $MBD2_{MBD}$ and $MBD2_{MBD+IDR}$ (**A**) The binding affinity for methylated DNA was determined by fluorescence polarization analysis for $MDB2_{MBD}$ and $MBD2_{MBD+IDR}$ with and without a thioredoxin (TRX) tag. Each titration shows evidence of non-specific binding to DNA at higher protein concentrations, typical of MBDs. We excluded these latter data points from the fit and normalized the data to 1.0. In addition, binding to methylated (mCpG) and unmethyated (CpG) DNA was measured for the full intrinsically disordered region, TRX-MBD2(IDR), that lacks the MBD. As expected, the IDR does not bind DNA in isolation. (**B**) ^{15}NH residual dipolar couplings ($^1D_{NH}$) were measured for $MBD2_{MBD+IDR}$ bound to methylated DNA and (**C**) fit to the known structure of the $MBD2_{MBD}$.

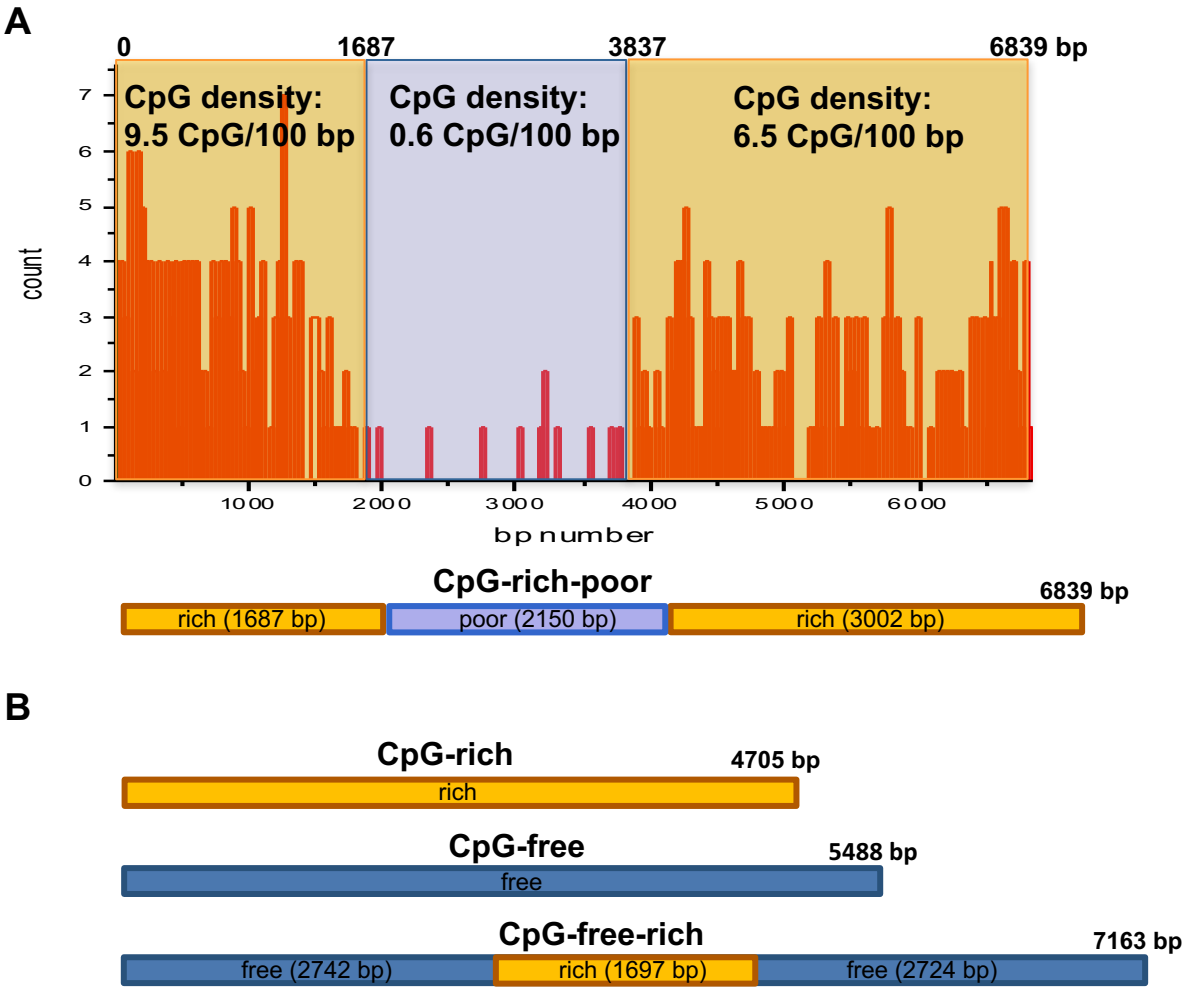

Supplementary Figure S2. Summary of the DNA substrates used for the DNA tightrope assay and AFM imaging. (**A**) The map and density of the CpG site on the CpG-rich-poor DNA substrate. (**B**) Diagrams of DNA substrates used for AFM imaging and in ligation reactions for the DNA tightrope assay. The linear CpG-rich DNA (4705 bp) was generated by restriction digestion with NcoI. The linear CpG-free and CpG-free-rich were obtained by restriction digestion of the plasmid DNA with StuI. DNA was purified using the Qiagen PCR kit.

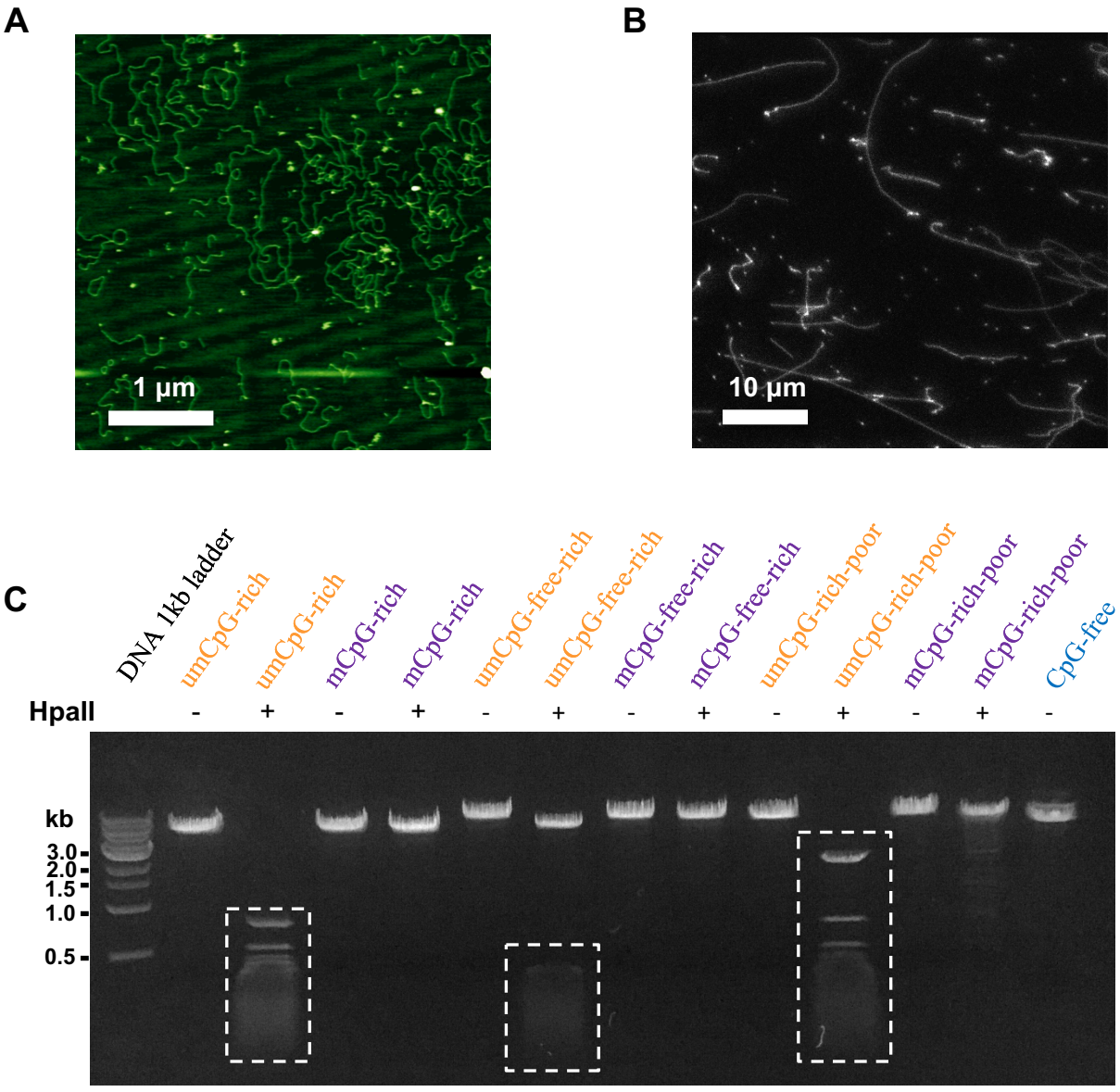

Supplementary Figure S3. Quantification of ligation and methylation efficiency. A representative (**A**) AFM image of ligated mCpG-rich DNA on a mica surface and **(B)** fluorescence image of YOYO1-stained ligated mCpG-rich DNA substrate on an APTES-treated cover slide. (**C**) Confirmation of DNA methylation through HpaII restriction digestion. The boxed regions indicate digested DNA fragments from unmethylated DNA.

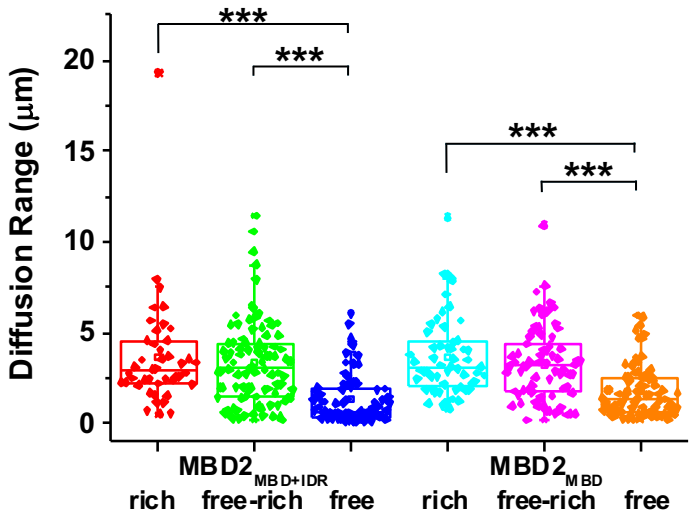

Supplementary Figure S4. Diffusion ranges of $MBD2_{MBD+IDR}$ and $MBD2_{MBD}$ on three DNA substrates. The diffusion range of $MBD2_{MBD+IDR}$ is 3.64 (±0.45) μm on CpG-rich, 3.32 (±0.23) μm on CpG-free-rich, and 1.31 (±0.13) μm on CpG-free. For $MBD2_{MBD}$, the diffusion range is 3.67 (±0.29) μm on CpG-rich, 3.27 (±0.24) μm on CpG-free-rich, and 1.77 (±0.15) μm on CpG-free. *: $p < 0.05$; **: $p < 0.005$; ***$p < 0.0005$.

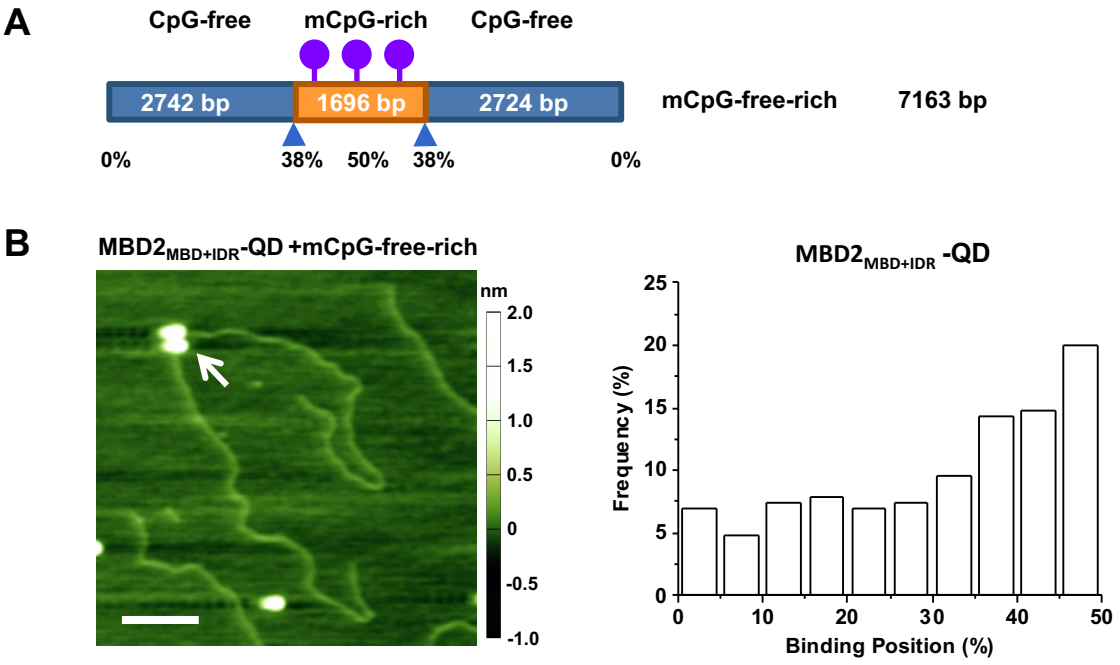

Supplementary Figure S5. QD-labeled $MBD2_{MBD+IDR}$ retains binding specificity for methylated CpG sites. (**A**) Cartoon drawing of the DNA substrate. (**B**) AFM imaging of $MDB2_{MBD+IDR}$-QD on linear mCpG-free-rich DNA substrate. Left panel: an AFM topographic image with a white arrow pointing to a $MBD2_{MBD+IDR}$-QD complex on DNA. The scale bar represents 200 nm. Right panel: the binding position of $MBD2_{MBD+IRD}$-QD complex on the linear mCpG-free-rich DNA substrate. Binding position analysis shows that over 49% of $MBD2_{MBD+IDR}$-QD (N=113 out of 230) binds to the methylated CpG-rich region (38% to 50% on mCpG-free-rich DNA).

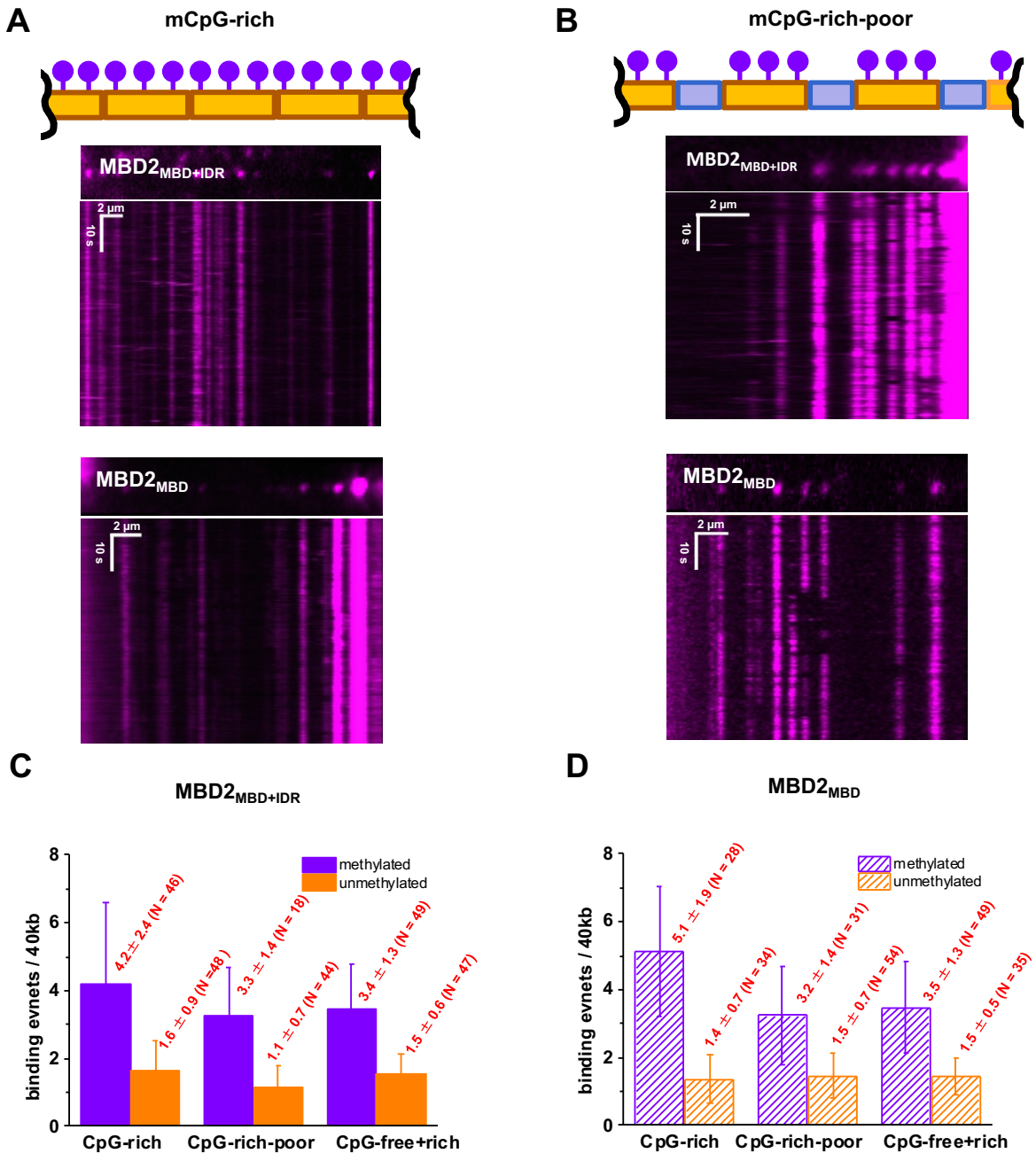

Supplementary Figure S6. Both $MBD2_{MBD+IDR}$ and $MBD2_{MBD}$ become static on methylated CpG-rich and CpG-rich-poor DNA substrates. (**A** and **B**) Top panels: cartoon drawing of the ligated DNA substrates using in the DNA tightrope assay. Middle and bottom panels: examples of individual DNA tightropes with QD-labeled proteins showing fluorescence images at the top and kymographs at the bottom. (**C** and **D**) The number of MBD2 complexes observed on DNA tightropes per 40 kb. The numbers in **C** ($MBD2_{MBD+IDR}$) and **D** ($MBD2_{MBD}$) report the mean±S.D. and the number of DNA tightropes analyzed. The average and SEM of the unmethylated and methylated DNA tightrope lengths are 12.3±0.4 μm (~38. 4 kb) and 11.1±0.3 μm (~34.7 kb), respectively.

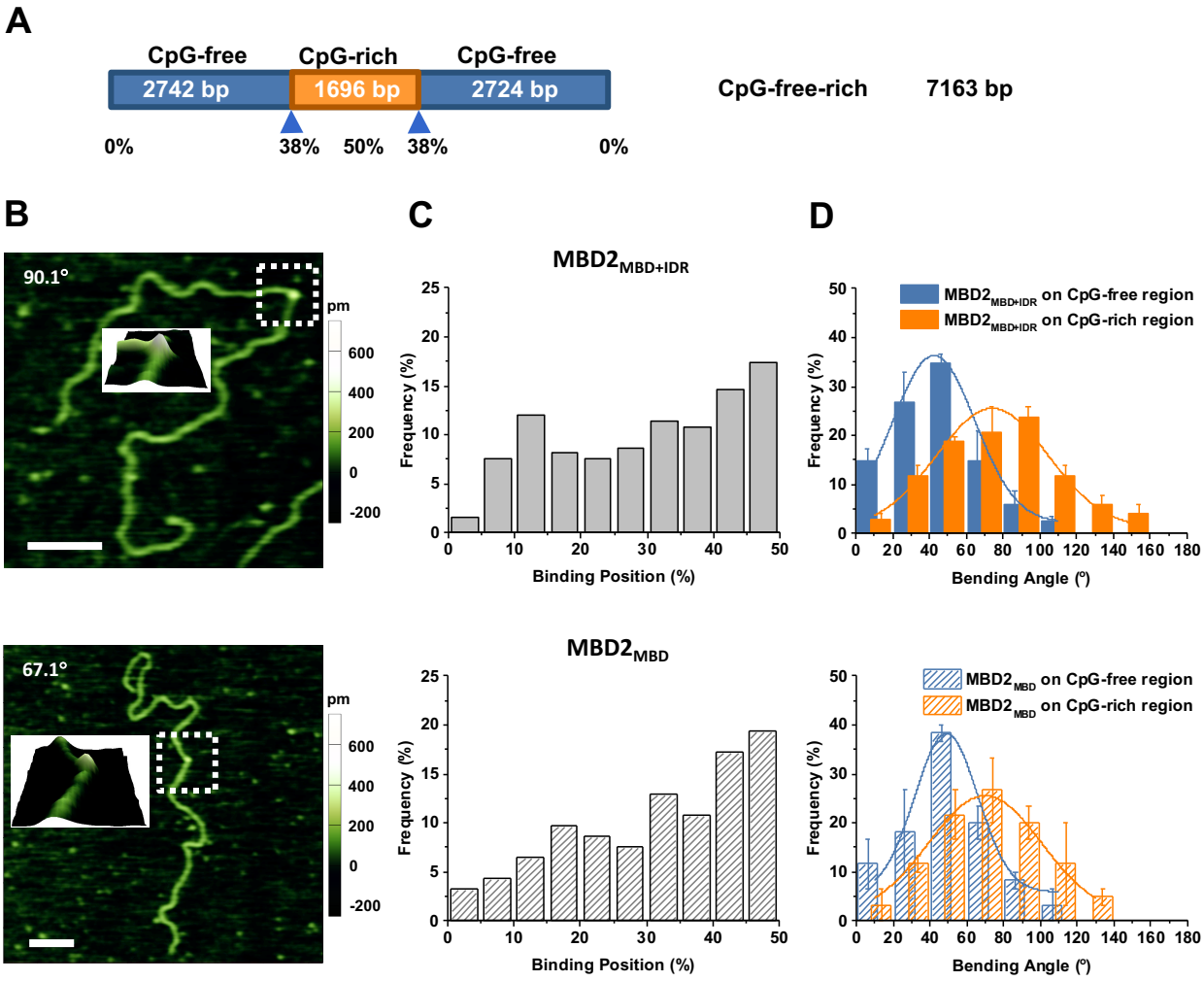

Supplementary Figure S7. Both $MBD2_{MBD+IDR}$ and $MBD2_{MBD}$ induce additional bending at the unmethylated CpG-rich region compared to binding at CpG-free regions. (**A**) Cartoon drawing of the CpG-free-rich DNA substrate. (**B**) AFM images of $MDB2_{MBD+IDR}$ (top panel) and $MBD2_{MBD}$ (bottom panel) on linear CpG-free rich substrate. The inserts show the 3D surface plots of the expanded (boxed) regions. The numbers in the images show the DNA bending angles at MBD binding sites. (**C**) Analysis of the binding position of $MDB2_{MBD+IDR}$ (top panel) and $MBD2_{MBD}$ (bottom panel) on linear CpG-free-rich substrate. Binding position analysis shows that over 42% of $MBD2_{MBD+IDR}$ (N = 79 out of 184) and 47% of $MBD2_{MBD}$ (N=44 out of 93) binds to the CpG-rich region (38% to 50%). (**D**) Analysis of the DNA bending angle induced by $MBD2_{MBD+IDR}$ and $MBD2_{MBD}$ at the CpG-free (0% to 38%) and CpG-rich regions (38% to 50%). The solid lines are Gaussian fits to the data (R^2> 0.97). The bending angles induced upon MBD protein binding are 42.5°±26.3° (N=113) and 74.1°±35.7° (N=76) for $MBD2_{MBD+IDR}$, 48.9°±20.1° (N=57) and 69.9°±36.1°(N=56) for $MBD2_{MBD}$ at CpG-free and CpG-rich regions, respectively.

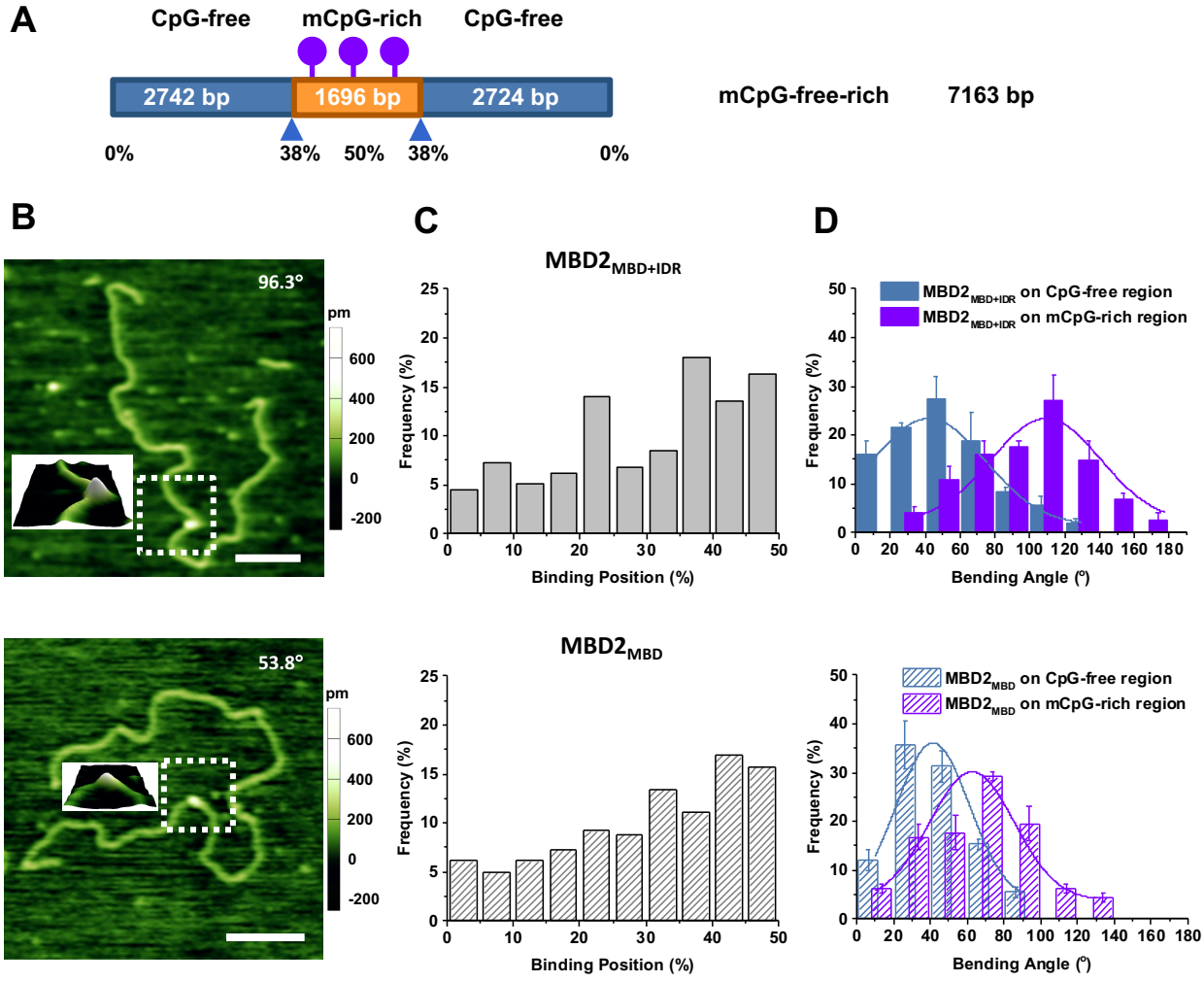

Supplementary Figure S8. Direct comparison of DNA bending upon binding of $MBD2_{MBD+IDR}$ and $MBD2_{MBD}$ to CpG-free and mCpG-rich regions in the mCpG-free-rich DNA substrate. (**A**) Cartoon drawing of the mCpG-free-rich DNA substrate. (**B**) AFM images of $MDB2_{MBD+IDR}$ (top panel) and $MBD2_{MBD}$ (bottom panel) on linear mCpG-free rich substrate. The inserts show the 3D surface plots of the expanded (boxed) regions. The numbers in the images show the DNA bending angles at MBD binding sites. (**C**) Analysis of the binding position of $MDB2_{MBD+IDR}$ (top panel) and $MBD2_{MBD}$ (bottom panel) on the linear mCpG-free-rich substrate. Binding position analysis shows that over 47% of $MBD2_{MBD+IDR}$ (N = 85 out of 178) and 43% of $MBD2_{MBD}$ (N=114 out of 260) binds to the methylated mCpG rich region (38% to 50%). (**D**) Analysis of the DNA bending angle induced by $MBD2_{MBD+IDR}$ and $MBD2_{MBD}$ at the CpG-free (0% to 38%) and mCpG-rich regions (38% to 50%). The solid lines in the right panels are Gaussian fits to the data (R^2 >0.90) with the peaks centered at 42.1°(±38.1°, N=105) at the CpG-free region and 102.2° (±41.3°, N=73) at the mCpG-rich region for $MBD2_{MBD+IDR}$, and 41.4° (±23.3°, N=181) at the CpG-free region and 62.6° (±27.6°, N=114) at the CpG-rich region for $MBD2_{MBD}$.

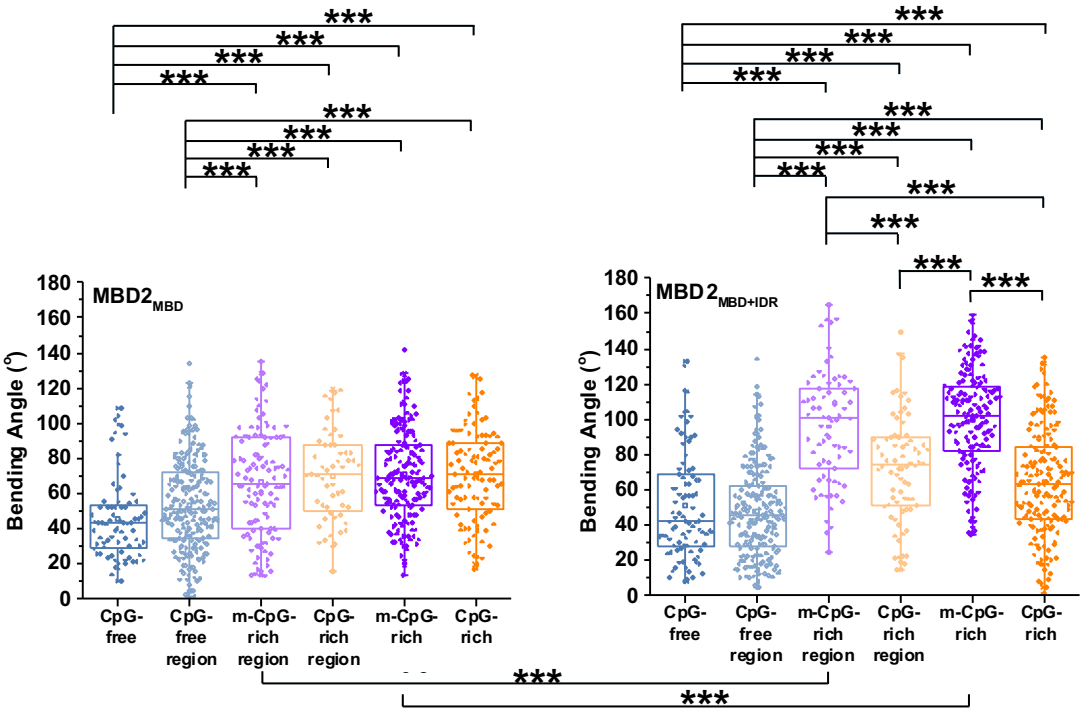

Supplementary Figure S9. Comparison of the DNA bending angles induced by MBD2. Box plots show the bending angles induced by binding of $MBD2_{MBD+IDR}$ and $MBD2_{MBD}$ to unmethylated and methylated CpG-free and CpG-rich DNA as well as the CpG-free and -rich regions within the CpG-free-rich DNA substrate. ***p < 0.0005. Significance values larger than 0.02 are not shown.

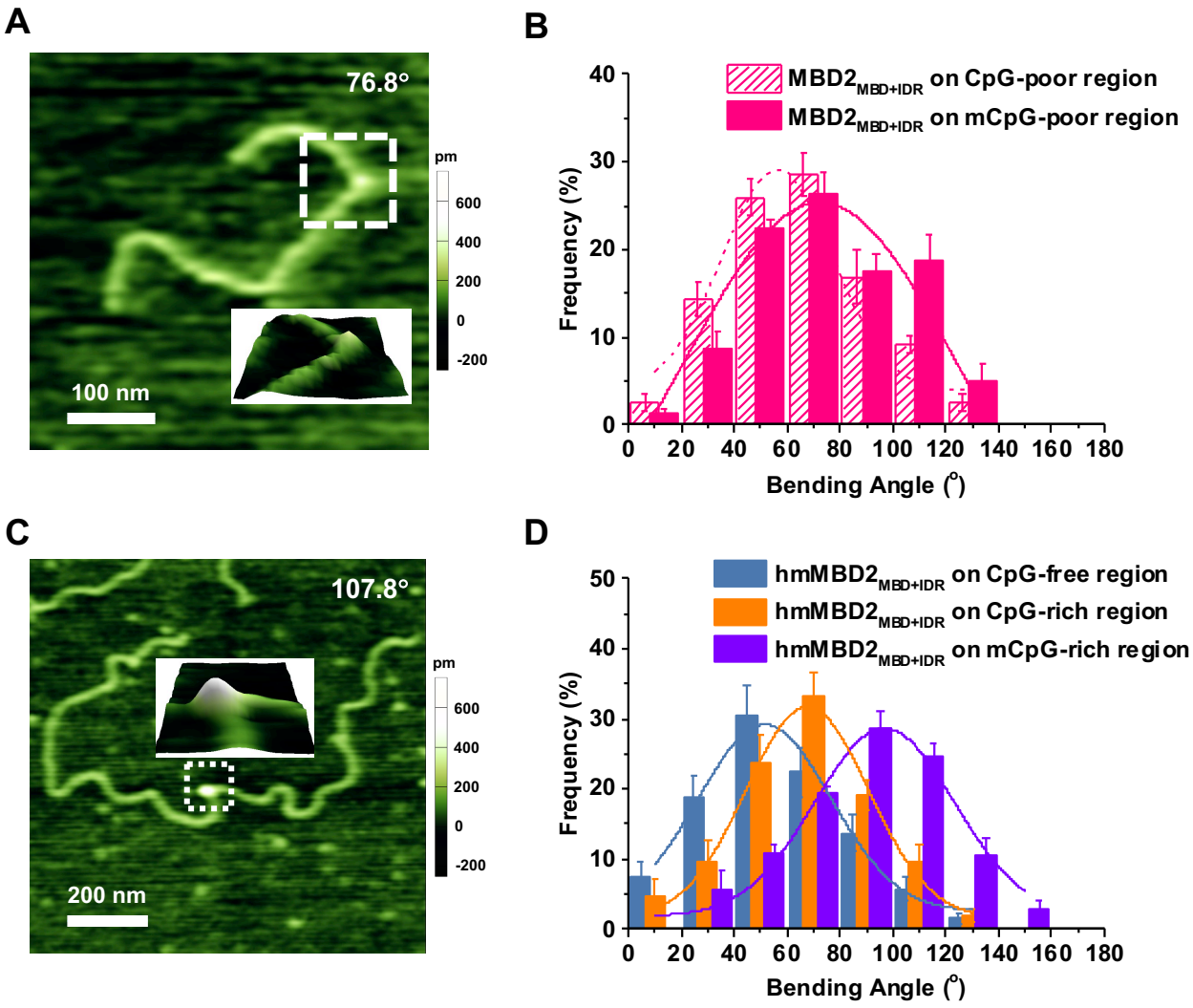

Supplementary Figure S10. $MBD2_{MBD+IDR}$ induces bending at the methylated CpG-poor region and hmMBD2 induces bending at unmethylated and methylated CpG-free-rich substrates. (**A**) An AFM image of $MDB2_{MBD+IDR}$ on the linear methylated CpG-poor substrate. The inserts show the 3D surface plots of the expanded (boxed) regions. The numbers in the images show the DNA bending angle at MBD binding site. (**B**) Analysis of the DNA bending angle induced by $MBD2_{MBD+IDR}$ at the CpG-poor and methylated CpG-poor regions. The bending angles induced upon MBD protein binding are 56.3°±24.7° (N=77) for CpG-poor and 72.4°±60.7° (N=80) for methylated CpG-poor. (**C**) An AFM image of human $MDB2_{MBD+IDR}$ on the linear methylated CpG-free-rich substrate. (**D**) Analysis of the DNA bending angle induced by human $MBD2_{MBD+IDR}$ at the CpG-free (51.5°±29.4°, N=121), CpG-rich (67.7°±27.2°, N=73) and methylated CpG-rich regions (96.8°±13.4°, N=102).